



Cite this: *RSC Chem. Biol.*, 2025, 6, 630

## Identification of $\gamma$ -butyrolactone signalling molecules in diverse actinomycetes using resin-assisted isolation and chemoenzymatic synthesis†

Yuta Kudo, <sup>a,b</sup> Keiichi Konoki b and Mari Yotsu-Yamashita b

Actinomycetes are prolific producers of secondary metabolites with diverse bioactivities. Secondary metabolism in actinomycetes is regulated by signalling molecules, often termed "bacterial hormones." In *Streptomyces griseus*, the  $\gamma$ -butyrolactone (GBL) A-factor (**1**) plays a key role in regulating secondary metabolism, including streptomycin production. The widespread presence of *afsA*, the gene encoding A-factor synthase, suggests that GBLs are a major class of signalling molecules in actinomycetes. However, their identification is hindered by the requirement for large-scale cultures. This study presents two methodologies for identifying natural GBLs. First, a resin-assisted culture method combined with MS-guided screening enabled the isolation and structural determination of GBLs (**2–5**) from smaller-scale cultures. Second, a chemoenzymatic synthesis method involving one-pot three enzymatic reactions was developed, allowing the production of GBL standards (**10a–10l**). Using these standards, HR-LC/MS analysis of 31 strains across 10 actinomycetes genera identified GBLs in nearly half of the tested strains, including genera where GBLs were detected for the first time. Chiral HPLC analysis further revealed the presence of the (3S)-isomer of GBL (**11**), an enantiomer of known GBLs. This study uncovers the widespread distribution and structural diversity of GBLs among actinomycetes, providing insights into their regulatory roles and potential for activating secondary metabolism, which may facilitate the discovery of new natural products.

Received 15th January 2025,  
Accepted 24th February 2025

DOI: 10.1039/d5cb00007f

[rsc.li/rsc-chembio](http://rsc.li/rsc-chembio)

## Introduction

Actinobacteria are a vital source of secondary metabolites with unique chemical structures and diverse biological activities, including antibiotic, antifungal, antitumour, and immunosuppressant activities.<sup>1</sup> These specialized metabolites have been developed into pharmaceuticals, beneficial chemicals, and biological probes. Owing to their remarkable metabolic versatility, actinomycetes are of great medical significance and remain an indispensable platform for drug discovery. Genome analyses have revealed that actinomycetes possess a vast yet largely untapped potential for secondary metabolite production. In recent years, the emergence and spread of antibiotic-resistant bacteria have become a global public health concern. Addressing this challenge requires a continuous supply of new antibiotics. Many antibiotics, including streptomycin, daptomycin, retapamulin, telavancin, ceftaroline fosamil, fidaxomicin and dalbavancin were produced

industrially *via* fed-batch fermentation of actinomycetes, which highlights their industrial significance, and importance of regulation of secondary metabolism.<sup>2–4</sup> Actinobacteria are also characterized by a complex life cycle that includes aerial mycelium and spore formation. Actinobacteria regulate these features, exhibiting exceptional secondary metabolism and morphological development, using low-molecular-weight signalling molecules. In *Streptomyces griseus*, the signalling molecule A-factor (**1**, Fig. 1) triggers secondary metabolism, including antibiotic streptomycin production and morphological differentiation, by activating a signalling pathway.<sup>5,6</sup> The A-factor is recognized by the receptor protein ArpA, which dissociates from DNA upon binding to the A-factor, leading to the expression of the central transcriptional activator AdpA. AdpA activates its regulons, including pathway-specific transcription factors for streptomycin biosynthesis genes and morphological differentiation.

Signalling molecules have been identified in *Streptomyces* species. The majority of known signalling molecules have 2,3-disubstituted  $\gamma$ -butyrolactone (GBL) structures (Fig. 1).<sup>6–11</sup> Other chemotypes, such as butanolide-type avenolide and SRB-1, as well as furan-type methylenomycin furan signalling molecules have also been identified.<sup>11–14</sup> Normal, iso- and anteiso-type fatty acid side chains in signalling molecules have been reported to have various chain lengths. In the case of GBL

<sup>a</sup> Frontier Research Institute for Interdisciplinary Sciences, Tohoku University, 6-3 Aramaki-Aza-Aoba, Aoba-ku, Sendai, Miyagi 980-8578, Japan.

E-mail: [yuta.kudo.d5@tohoku.ac.jp](mailto:yuta.kudo.d5@tohoku.ac.jp)

<sup>b</sup> Graduate School of Agricultural Science, Tohoku University, 468-1 Aramaki-Aza-Aoba, Aoba-ku, Sendai, Miyagi 980-8572, Japan

† Electronic supplementary information (ESI) available. See DOI: <https://doi.org/10.1039/d5cb00007f>



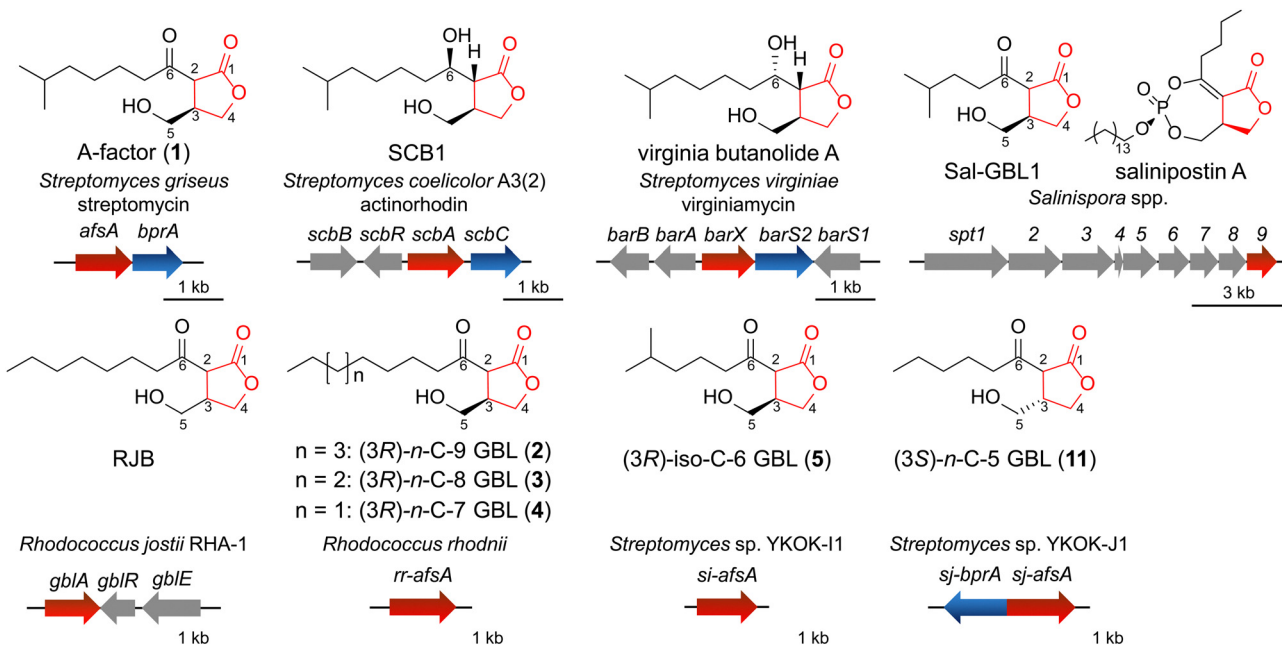


Fig. 1 Chemical structures of  $\gamma$ -butyrolactone (GBL)-containing natural compounds along with their producers, secondary metabolites, and relevant biosynthetic genes. Compounds **2–5** and **11** were identified in this study. *afsA* homologues are highlighted in red, *bprA* homologues are highlighted in blue, and others are highlighted in grey.

signalling molecules, the 6-keto GBLs, which includes the A-factor (**1**), and the 6-hydroxy GBLs, represented by SCB1 in *Streptomyces coelicolor* A3(2), have been reported. Both (6*R*) and (6*S*) stereochemistry have been reported in 6-hydroxy GBLs (Fig. 1). All GBL signalling molecules with defined stereochemistry have been reported in the (3*R*)-form, although some early papers illustrated (3*S*)-form GBL structures without experimental verification. The stereochemistry at the C-2 position of 6-keto GBLs is uncertain due to the occurrence of epimerization *via* keto-enol tautomerization. Signalling molecules have been less commonly identified in genera other than *Streptomyces*. Kudo *et al.* identified GBLs in the marine actinomycete *Salinipostia* spp.<sup>15</sup> A GBL named RJB was identified in *Rhodococcus jostii* RHA-1 using LCMS, but the stereochemistry at C-3 in RJB was not determined.<sup>16</sup> The signalling molecule B-factor has been reported in *Nocardia*,<sup>17</sup> but no GBLs have been confirmed.

The A-factor is biosynthesized by the key biosynthetic gene *afsA*, which encodes A-factor synthase (AfsA). Homologues of *afsA* are widely distributed among actinomycetes.<sup>11</sup> Although signalling pathways vary among species,<sup>5,18–21</sup> they share a common feature: the initial recognition of signalling molecules by specific receptors. Early studies suggested that GBL induces secondary metabolite production in various *Streptomyces* species.<sup>22–25</sup> Bioinformatic analysis further suggested that approximately 60% of *Streptomyces* strains are capable of producing GBL-type compounds.<sup>26</sup> Despite their significance, only a limited number of signalling molecules have been structurally characterized. Actinomycetes represent a vast group of microorganisms encompassing numerous genera, with the genus *Streptomyces* alone comprising over 1000 species. However, fewer than 20 GBLs have been unambiguously identified using analytical chemistry

methods such as NMR and high-resolution liquid chromatography-mass spectrometry (HR-LCMS).<sup>11</sup> Signalling molecules are typically produced in low quantities, possibly because they act *in vivo* at nanomolar concentrations (e.g.,  $10^{-9}$  M for the A-factor). Conventional methods for isolation and structural elucidation require immense effort. The isolation of known signalling molecules often involves the processing of hundreds of litres of liquid cultures of actinomycetes. Notable examples include the isolation of SCB1 from 300 litres,<sup>8</sup> *virginiae* butanolide A from 1150 litres,<sup>27</sup> and IM-2 from 1150 litres of culture.<sup>28</sup> The significant effort required for the identification of signalling molecules may explain why many signalling molecules remain unidentified. While these molecules are critical regulatory factors, no practical and universally applicable methods currently exist for their systematic identification. As a result, knowledge of their chemical structures and distribution among actinomycetes is still limited.

The biosynthetic pathway of the A-factor (**1**) has been elucidated primarily through *in vitro* reactions involving AfsA, butanolide phosphate reductase (BprA), and phosphatase.<sup>29</sup> In this pathway, AfsA catalyses the condensation of dihydroxyacetone phosphate (DHAP) and  $\beta$ -ketoacyl-ACP (acyl carrier protein), followed by spontaneous aldol condensation to form butenolide phosphate. Subsequently, BprA reduces the double bond between C-2 and C-3, resulting in the formation of GBL phosphate. The final step involves dephosphorylation, producing the GBL A-factor (**1**). A homologue of AfsA, ScbA, performs a similar function in *S. coelicolor* A3(2), catalysing the biosynthesis of SCB1.<sup>30</sup> Another homologue, MmfL, is employed in the biosynthesis of methylenomycin furan, even though the chemical structures of the final products differ.<sup>31</sup> The biosynthesis of salinipostin, a highly unusual phosphotriester compound with antimalarial activity, also



begins with the formation of a GBL structure catalysed by an *AfsA* homologue, *Spt9*.<sup>15</sup> Additionally, GBLs such as Sal-GBL1 and Sal-GBL2 have been detected in salinipostin-producing *Salinispore* strains.<sup>15</sup> These strains also produce volatile GBL compounds, known as salinilactones, which exhibit cytotoxicity.<sup>32–34</sup> As shown in previous analyses, the *qfA* gene not only is essential for the biosynthesis of GBLs but also plays a critical role in the production of related compounds. The *qfA* gene in each strain may also accept different  $\beta$ -ketoacyl-ACPs. With respect to the synthesis of GBL, the first asymmetric total synthesis of the A-factor was achieved by Mori in 1981.<sup>35–37</sup> Brown *et al.* later reported an efficient biomimetic racemic synthesis of the A-factor,<sup>38</sup> and Parkinson *et al.* recently demonstrated the asymmetric synthesis of SCBs.<sup>39</sup>

The fatty acyl chain structure, 6-hydroxy group, and stereochemistry of signalling molecules are rigorously recognized by the *ArpA* receptor. Actinomycete signalling molecules, such as the A-factor and SCBs, are commonly considered species-specific due to their high receptor specificity and are often referred to as “bacterial hormones.” These molecules have been studied for their regulatory function in producer strains and closely related strains. However, some studies have shown that signalling molecules can influence secondary metabolism in nonproducer strains. For example, supplementation with SCBs induced paulomycin production in *Streptomyces albus*,<sup>40</sup> and butenolides stimulated avermectin production in *Streptomyces avermitilis*.<sup>41</sup> Recently, actinomycete signalling molecules have been reported to activate quorum sensing in Gram-negative bacteria and enhance secondary metabolite production.<sup>42</sup> These findings suggest that actinomycetes utilize signalling molecules not only as self-inducing regulators but also as potential chemical tools for interspecies communication. On the other hand, the addition of plant hormones has been reported to induce antibiotic actinorhodin production in *Streptomyces*, implying that signalling pathways may be influenced by chemical signals from other organisms.<sup>43</sup> In the field of synthetic biology, the artificial construction of

signalling pathways has garnered attention as a promising tool for developing regulatory systems.<sup>44–46</sup>

Given the specific ability of signalling molecules to regulate secondary metabolism and morphological development, identifying such molecules in individual species is crucial for understanding and controlling the production of natural compounds in actinomycetes. While most research on signalling molecules has focused on the genus *Streptomyces*, studies on other genera remain limited, as described above. Nevertheless, actinomycetes outside the genus *Streptomyces* are also known to produce valuable secondary metabolites. For example, antitumour compounds tested in clinical trials, such as salinosporamide and rebeccamycin, were isolated from the genera *Salinispore* and *Lentzea* (formerly designated *Nocardia*), respectively.<sup>47–49</sup> Anti-trypanosomal macrolides actinoallolides were found in the endophytic actinomycete *Actinoallomorus*.<sup>50,51</sup> These examples demonstrate that actinomycetes other than *Streptomyces* are also promising sources of bioactive natural compounds. Approaches such as cocultivation<sup>52</sup> and heterologous expression<sup>53–56</sup> have been demonstrated to be effective in activating dormant secondary metabolism and discovery of the new natural compounds. However, actinomycetes still possess largely untapped potential for secondary metabolism, and exploring strategies to harness this potential remains a critical challenge. Understanding the signalling molecules in a broad range of actinomycetes is fundamental for unlocking their metabolic potential and optimizing the production of beneficial compounds. The use of signalling molecules to activate silent secondary metabolic pathways would represent a viable strategy for discovering new natural products, potentially paving the way for resupplying novel pharmaceuticals derived from actinomycetes.

In this study, we aimed to establish a methodology for the rapid identification of GBLs, which are major signalling molecules in actinomycetes (Fig. 2). Our first objective was to achieve efficient isolation and structural determination of GBLs

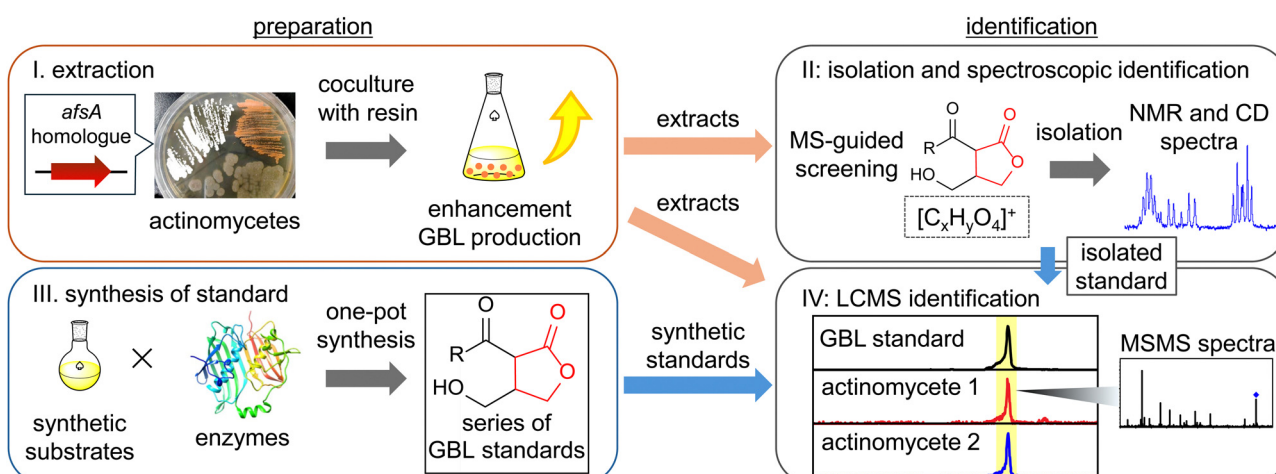


Fig. 2 Overview of identification methods for  $\gamma$ -butyrolactone (GBL) in actinomycetes. (I) Extraction of natural GBLs from *afsA* homologue-harbouring actinomycete cocultured with resin. (II) MS-guided screening, isolation, and spectroscopic identification of natural GBLs. (III) Chemoenzymatic synthesis of GBLs for the preparation of LCMS standards. (IV) Identification of GBLs in actinomycete using HR-LCMS and MS/MS with synthetic and isolated standards. Chiral HPLC analysis is applicable for determining absolute configurations.



without culturing hundreds of litres of actinomycetes. Over the past few decades, mass spectrometry (MS)-guided screening has become a practical and widely employed technique in natural product chemistry.<sup>57–60</sup> We cocultured actinomycetes with absorbent resin to enhance GBL production and subjected the extracts to MS-guided screening focused on the GBL structure. This approach enabled the isolation and structural determination of GBLs (2–5) as new natural products from a culture volume of less than 7.5 litres. To further accelerate the identification process, we developed a concise chemoenzymatic synthesis method for synthesizing a series of GBLs with varying side chain structures. Using both the synthesized and isolated GBLs, we analysed extracts from 31 strains across 10 actinomycete genera with HR-LCMS, revealing the widespread occurrence of GBLs among diverse actinomycetes. Unexpectedly, a GBL isolated from *Streptomyces* sp. YKOK-I1 was identified as the (3*S*)-*n*-C-5 GBL (11), marking the first experimental confirmation of (3*S*)-isomer of GBL. This study expands our understanding of the chemical diversity and distribution of GBLs in actinomycetes, providing insights into their metabolic potential and role as regulatory molecules.

## Results and discussion

### Resin-assisted isolation and structure determination of $\gamma$ -butyrolactone compounds

We cocultured actinomycetes with resin and subjected the crude extracts to MS-guided screening to rapidly identify GBL compounds. GBLs were isolated from the actinomycetes showing significant production, and their structures, including their absolute stereochemistry, were determined. A total of 31 strains were analysed in this study (Table S1, ESI<sup>†</sup>). We first selected the actinomycetes containing *qfsA* homologues (pairwise AA similarity >30%) from various genera, including *Streptomyces*, *Nocardia*, *Rhodococcus*, *Kutzneria*, *Gordonia*, *Kitasatospora*, *Dietzia* and *Salinispora*, which were obtained from bacterial collections. As described above, the salinipostin biosynthetic gene cluster (*spt*) corresponds to the production of GBLs;<sup>11,15,61</sup> therefore, 14 strains containing an *spt*-like biosynthetic gene cluster were included. Strains lacking high-similarity *qfsA* homologues were also selected from the *Mycobacterium* and *Mycolicibacterium* genera. Five *Streptomyces* strains were isolated from soil collected in Okinawa, Japan, and were also subjected to analysis. The 16S rRNA sequences of these strains were amplified via PCR and analysed, and the whole genomes of the two strains were sequenced via next-generation sequencing (NGS). In a previous study, GBL production in marine actinomycete *Salinispora* strains was enhanced by cocultivation with the absorbance resin Amberlite XAD7HP (Sigma-Aldrich).<sup>15,62</sup> Although definitive evidence is lacking, it is presumed that the resin enhances GBL production in actinomycetes by adsorbing GBL in the culture. Based on those findings, the 31 strains representing 10 genera from 6 families were fermented in liquid media with XAD7HP resin. The cells and resin were extracted with acetone and pretreated with a C-18 SPE column. Eluent fractions were analysed using HR-LCMS in positive and negative ion modes, and the *m/z* values corresponding to

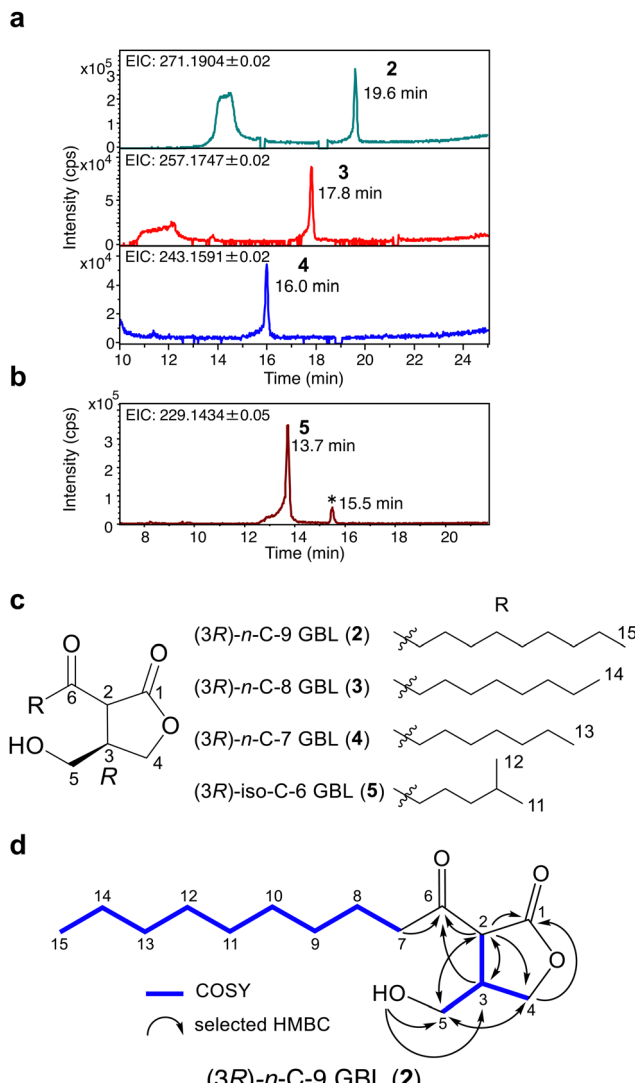


Fig. 3 Screening and structural analysis of natural  $\gamma$ -butyrolactones (GBLs, 2–5). (a) LCMS chromatograms of the extract of *Rhodococcus rhodnii*. (b) LCMS chromatograms of the extract of *Streptomyces* sp. YKOK-I1. A peak marked with an asterisk correspond to compounds whose exact masses differ from those of GBLs. (c) Chemical structures of 2–5. (d) Observed COSY correlations and selected HMBC correlations in 2.

$[\text{C}_x\text{H}_y\text{O}_4]^+$  and  $[\text{C}_x\text{H}_y\text{O}_4]^-$  were detected. As a result, notable peaks (2–4) were detected in *Rhodococcus rhodnii* JCM 3203, and peak (5) was detected in the isolated *Streptomyces* sp. YKOK-I1 (5) (Fig. 3a and b). These potential GBLs were then subjected to isolation and spectroscopic analysis.

Compound 2 was extracted with acetone from a 2.5 litres culture of *R. rhodnii* JCM 3203 fermented with resin and isolated using a Cosmosil 140C18-OPN column and an Inert-Sustain C18 column (2: 0.30 mg). GBLs 3 and 4 were obtained from an additional long-term 5 litres culture of *R. rhodnii* JCM 3203 and then purified using a similar method. The isolation of 3 and 4 was achieved with a Kinetex XB-C18 column (3: 0.15 mg, 4: 0.11 mg). The molecular formulae of these compounds were determined to be  $\text{C}_{15}\text{H}_{26}\text{O}_4$  (2),  $\text{C}_{14}\text{H}_{24}\text{O}_4$  (3) and  $\text{C}_{13}\text{H}_{22}\text{O}_4$  (4) on the basis of their ESI-TOF-MS monoisotopic peaks,

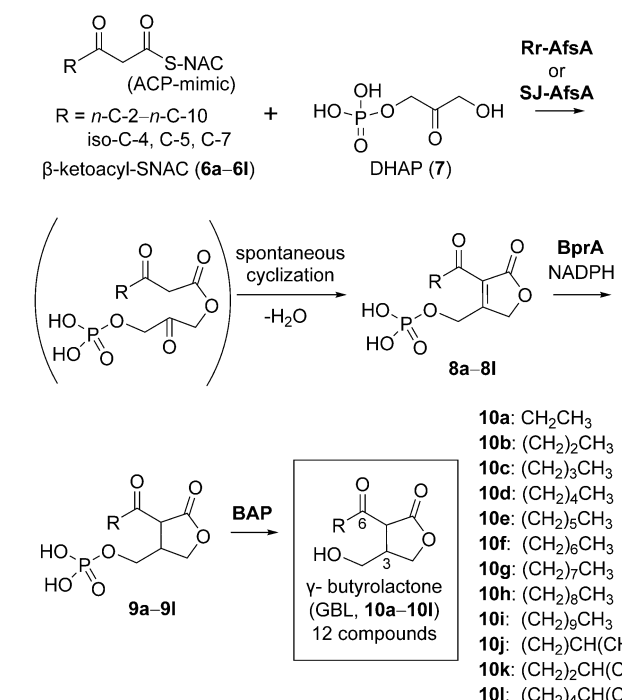


suggesting side chains C-9, C-8, and C-7, respectively (Fig. S1–S4, ESI†). The  $^1\text{H}$  NMR spectrum of **2** in  $\text{CDCl}_3$  showed diagnostic double triplet signals at  $\delta_{\text{H}}$  2.99 and 2.64 ppm (Fig. S67 and S68, ESI†). The methyl triplet signal at  $\delta_{\text{H}}$  0.88 indicated the presence of a *n*-alkyl side chain. Signal sets derived from keto–enol tautomerization were also observed. 2D NMR (COSY, TOCSY, HSQC, and HMBC) clarified the planar structure of **2** (Fig. 3 and Fig. S69–S72, ESI†). All the proton and carbon signals in the major keto form were assigned (Table S2, ESI†). Similarly, the structures of **3** and **4** were characterized using 1D- and 2D-NMR spectra (Fig. S73–S84, Tables S3 and S4, ESI†). Compounds **3** and **4** resemble GBL structures and contain *n*-octyl and *n*-heptyl chains, respectively (Fig. 3). The absolute configurations of these compounds were analysed using CD spectroscopy. Compound **2** displayed positive Cotton effects (284 nm,  $\Delta\epsilon + 0.446$ , 218 nm,  $\Delta\epsilon + 0.265$ , Fig. S6, ESI†), closely resembling the (3*R*)-A-factor (283.5 nm,  $\Delta\epsilon + 0.699$ , 221.0 nm,  $\Delta\epsilon + 0.420$ ).<sup>35,37</sup> Thus, **2** was assigned as (3*R*)-*n*-C-9 GBL (Fig. 3), the longest side-chain natural GBL known to date. Compounds **3** and **4** were assigned as (3*R*)-*n*-C-8 GBL and (3*R*)-*n*-C-7 GBL, respectively, on the basis of their CD spectra (Fig. S7 and S8, ESI†). Compound **5** was isolated from a 5 litres culture of *Streptomyces* sp. YKOK-I1 fermented with resin (**5**, 0.15 mg). The molecular formula of **5** was determined to be  $\text{C}_{12}\text{H}_{20}\text{O}_4$  (**5**) on the basis of the monoisotopic peaks in the ESI-TOF-MS data, suggesting a C-6 side chain (Fig. S1 and S5, ESI†). NMR analysis revealed a planar structure, and CD analysis confirmed a (3*R*)-configuration (Fig. 3, Fig. S9 and S85–S90, ESI†). Compounds **2** and **3** represent the first naturally occurring 6-keto GBLs with these side chain lengths. A compound with an *n*-C-7 side chain, which was identified *via* LCMS with a racemic synthetic standard, was previously reported as RJB in *Rhodococcus jostii* RHA-1.<sup>16</sup> However, this RJB was not analysed using NMR, and the absolute configuration was not investigated. Compound **5** has been reported to be a biosynthetic intermediate of virginiae butanolide A, a signalling molecule in *S. virginiae*,<sup>63</sup> but was first isolated as a natural product from *Streptomyces* sp. YKOK-I1. HR-LCMS analysis confirmed that *Streptomyces* sp. YKOK-I1 lacked any possible peaks for virginiae butanolide A.

Using an MS-guided screening method combined with resin fermentation, we successfully achieved concise identification of new natural GBLs from small-scale cultures of actinomycetes. This method provides solutions to the challenges faced in previous studies, which required the processing of hundreds of litres of cultures to isolate GBLs. In addition to the identified GBLs, potential natural GBL compounds were detected in the actinomycetes extracts during screening. While most known GBL compounds are 6-hydroxy GBLs, our results suggest that 6-keto GBL compounds are more widely distributed than previously recognized. Despite enhanced production through resin cocultivation, the amount of GBLs in some extracts was estimated to be insufficient for NMR and CD analysis based on the peak intensities. In addition, in *Streptomyces* sp. YKOK-I1 (Fig. S10, ESI†), the GBL yield was notably lower in 500 mL cultures ( $N = 2$ ) than in 50 mL small-scale cultures, which presented high concentrations of GBLs ( $N = 4$ ).

## Chemoenzymatic synthesis of GBL compounds

MS-guided screening suggested a wide distribution of 6-keto GBL compounds. To expand the rapid identification methodology, we synthesized a series of 6-keto GBL compounds *via* a chemoenzymatic approach (Scheme 1). Previous studies have reported the biomimetic racemic synthesis of the A-factor.<sup>38</sup> Horinouchi *et al.* reported key reactions catalysed by AfsA and BprA in the A-factor biosynthetic pathway. In recent years, technological advancements in enzyme structure prediction and heterologous expression of enzymes have facilitated the development of enzyme-mediated synthesis of natural products and pseudo-natural products.<sup>64–66</sup> In this study, we performed enzymatic reactions using the AfsA homologues, BprA and phosphatase with synthesized substrate mimics. Docking models were constructed using AutoDock Vina<sup>67,68</sup> to evaluate the interaction between the AfsA homologue protein structures generated by AlphaFold2<sup>69</sup> and  $\beta$ -ketoacyl-*N*-acetyl cysteamine (SNAC) substrates, which serve as mimics of  $\beta$ -ketoacyl-ACP. On the basis of this *in silico* analysis, two AfsA homologues, *rr-afsA* from *R. rhodnii* 3203 and *sj-afsA* from *Streptomyces* sp. YKOK-J1, were selected as biocatalysts (Fig. S11, ESI†). *rr-afsA* was expected to recognize substrates with long *n*-acyl chains. On the basis of the LCMS analysis (Fig. S10, ESI†), *Streptomyces* sp. YKOK-J1 was estimated to produce *n*- and iso-C-5 GBL; therefore, SJ-AfsA might recognize substrates with branched and middle-length acyl chains. However, *sj-afsA* showed low sequence homology with AfsA in *S. griseus* (Table 1). Similarly, based on the docking model, it was predicted that the known BprA in *Streptomyces griseus*<sup>29</sup> recognizes various butanolide phosphates as substrates (Fig. S11, ESI†). *rr-afsA*, *sj-afsA*, and *bprA* were cloned into pET28a and



**Scheme 1** Chemoenzymatic synthesis of 6-keto  $\gamma$ -butyrolactones (**10a–10l**) using three types of enzymes.



Table 1 Distribution of  $\gamma$ -butyrolactones (GBLs) in 31 strains of actinomycetes

Actinomycete species	Strain	Detected GBLs <sup>f</sup>	AfsA homolog similarity (%) <sup>h</sup>
<i>Dietzia timorensis</i>	NBRC 104184	<b>10f, 10g, 10h</b>	33.7
<i>Gordonia polyisoprenivorans</i>	JCM 10675	<b>10f, 10g, 10h</b>	35.9
<i>Kitasatospora cheerisanensis</i>	JCM 21757		38.0
<i>Kutzneria albida</i>	JCM 3240		38.6
<i>Mycobacterium cookii</i>	JCM 12404		16.8
<i>Mycolicibacterium austroafricanum</i>	JCM 13017		23.2
<i>Mycolicibacterium chlorophenolicum</i>	JCM 7439		24.6
<i>Nocardia anaemiae</i>	JCM 12396	<b>10h</b>	32.9
<i>Nocardia carnea</i>	JCM 30727	<b>10h</b>	38.8
<i>Nocardia hareniae</i>	JCM 14548	<b>10f, 10h</b>	35.8
<i>Nocardia lijiangensis</i>	JCM 13592	<b>10h</b>	37.6
<i>Nocardia pseudovaccinii</i>	JCM 11883		33.8
<i>Nocardia tenerifensis</i>	JCM 12693		35.0
<i>Nocardia xishanensis</i>	JCM 12160	<b>10h, 10l</b>	35.5
<i>Rhodococcus erythropolis</i>	NBRC 15567		24.3
<i>Rhodococcus jostii</i> RHA-1	NBRC 108803	<b>10f (RJB)<sup>16</sup>, 10g</b>	39.9
<i>Rhodococcus rhodnii</i>	JCM 3203	<b>2, 3, 4, 10i</b>	42.4
<i>Rhodococcus rhodochrous</i>	NBRC 16069	<b>10d, 10e, 10f, 10g, 10h</b>	38.0
<i>Salinispora tropica</i>	JCM 13857	<b>10c</b> (Sal-GBL2), <b>10j, 10k</b> (Sal-GBL1) <sup>15</sup>	36.7
<i>Streptomyces capuensis</i>	JCM 4460		49.2
<i>Streptomyces durhamensis</i>	JCM 4291		51.9
<i>Streptomyces viridosporus</i> ( <i>S. ghanaensis</i> )	JCM 4963		44.1
<i>Streptomyces griseoaurantiacus</i>	JCM 4763		28.2
<i>Streptomyces griseus</i>	NBRC 12875	A-factor ( <b>1</b> ), <b>5<sup>g</sup></b> , <b>10d, 10e, 10f, 10k</b>	-
<i>Streptomyces rimosus</i> subsp. <i>rimosus</i>	JCM 4073		49.2
<i>Streptomyces coelicolor</i> A3(2) ( <i>S. violaceoruber</i> )	NBRC 15146	6-hydroxy GBLs (SCBs)	73.2
<i>Streptomyces</i> sp. <sup>a)</sup>	YKOK-D1	6-hydroxy GBLs	NA <sup>i</sup>
<i>Streptomyces</i> sp. <sup>b)</sup>	YKOK-F1		NA <sup>i</sup>
<i>Streptomyces</i> sp. <sup>c)</sup>	YKOK-G2b	<b>10d, 5<sup>g</sup>, 10f, 10g, 10h, 10k, 10l</b>	NA <sup>i</sup>
<i>Streptomyces</i> sp. <sup>d)</sup>	YKOK-I1	<b>5, 10d, 10f, 10k, 10l</b>	54.5
<i>Streptomyces</i> sp. <sup>e)</sup>	YKOK-J1	<b>5<sup>g</sup>, 10f, 10k, 11</b>	26.2

<sup>a</sup> Partial 16S rRNA sequence shows 100% identity with *Streptomyces wuyuanensis*. <sup>b</sup> Partial 16S rRNA sequence shows 100% identity with *Streptomyces sporoverrucosus* and some *Streptomyces* spp. <sup>c</sup> Partial 16S rRNA sequence shows 99.8% identity with *Streptomyces cinereoruber* subsp. fructofermentans. <sup>d</sup> Whole 16S rRNA sequence shows 98.8% identity with *Streptomyces acidiscabies*. <sup>e</sup> Whole 16S rRNA sequence shows 98.6% identity with *Streptomyces cyaneochromogenes*. <sup>f</sup> Strains with AfsA homology higher than 30% but no detectable GBL are shown in blue. <sup>g</sup> iso-C-6 GBL was detected, although its absolute configuration was not determined. <sup>h</sup> Strains with AfsA homology higher than 30% are shown in yellow. <sup>i</sup> Genome sequence was not available.

pET28-MBP-TEV<sup>70</sup> vectors. With these constructs, three enzymes were heterologously expressed in *E. coli* and then purified using Ni-NTA affinity chromatography (Fig. S12, ESI<sup>†</sup>). Twelve  $\beta$ -ketoacyl-SNAC substrates (**6a–6l**), mimics of the substrate  $\beta$ -ketoacyl-ACP, were prepared *via* concise organic synthesis (see ESI<sup>†</sup>). Another substrate, DHAP (7), was purchased or synthesized. With the substrates and enzymes in hand, *in vitro* enzymatic reactions were conducted. Both MBP-Rr-AfsA and MBP-SJ-AfsA gave possible butenolide phosphate products (**8**, Fig. S13, ESI<sup>†</sup>) with exact masses matching the expected values (substrate: *n*-C-4  $\beta$ -ketoacyl-SNACs (**6c**), *m/z* 277.0481,  $[M - H]^-$  calcd. 277.0483). However, the products were unstable.<sup>15</sup> Chemical reduction of the C-C double bond in butenolide phosphate with NaBH<sub>3</sub>CN yielded relatively stable products (*m/z* 279.0644,  $[M - H]^-$  calcd. 279.0639), estimated to be GBL phosphate (**9**, Fig. S13, ESI<sup>†</sup>).

Considering the instability of butenolide phosphate (**8**), we adopted successive enzymatic reactions to avoid handling unstable butenolide intermediates. A reaction with AfsA was performed, followed by a reaction with BprA and the cofactor NADPH. LCMS analysis using C-18- and C-8-reversed-phase columns confirmed that all the tested substrates were converted into corresponding GBL-phosphates (**9**) *via* successive MBP-Rr-AfsA and MBP-BprA enzymatic reactions (Fig. S14–S26, ESI<sup>†</sup>). Compared with Rr-AfsA, SJ-AfsA exhibited narrower substrate tolerance, but higher conversion rates were observed with *n*-C-4, *n*-C-5, and iso-C-5 side chain substrates (Table S6, ESI<sup>†</sup>). Since compounds **2–4** were identified in *R. rhodnii*, the genuine substrates of Rr-AfsA are likely to have these chain lengths. However, Rr-AfsA showed higher conversion efficiency for substrates with shorter chain lengths under the reaction condition (25 °C for 1 h).



This discrepancy might be attributed to the low solubility of the  $\beta$ -ketoacyl-SNAC substrate (**6**) in the reaction buffer. In line with the natural compound profile of *Streptomyces* sp. YKOK-J1 (Fig. S10, ESI<sup>†</sup>), SJ-AfsA accepted substrates with *n*- and iso-C-5 side chains and similar substrates. However, substrates with longer side chains were poorly converted into the corresponding phosphates by SJ-AfsA (Table S6, ESI<sup>†</sup>), probably due to the spatial constraints in the binding pocket of SJ-AfsA. MBP-BprA reduced all the tested butenolide to butyrolactone, although substrate specificity was not evaluated in detail in this study because of the instability of the butanolide substrate under the reaction conditions.

The AfsA and BprA reaction products, GBL phosphates (**9**), were subjected to dephosphorylation using a commercially available bacterial alkaline phosphatase (BAP). Dephosphorylation of all the tested GBL-phosphates was confirmed by detecting their exact masses *via* LCMS (Fig. S27–S38, ESI<sup>†</sup>). Exploiting the substrate capability of the two AfsA, BprA, and BAP enzymes, we synthesized twelve 6-keto GBL compounds with side chains, including *n*-C-2, *n*-C-3, *n*-C-4, *n*-C-5, *n*-C-6, *n*-C-7, *n*-C-8, *n*-C-9, *n*-C-10, *iso*-C-4, *iso*-C-5 and *iso*-C-7 side chains (Fig. 4, **10a–10l**).

Next, we developed a one-pot chemoenzymatic synthesis of GBLs using three successive enzymatic reactions involving AfsA, BprA, and BAP. The reaction began with *n*-C-5  $\beta$ -ketoacyl-SNAC (**6d**) and DHAP (**7**) incubated with MBP-SJ-AfsA. To this mixture,

MBP-BprA, NADPH, and MgCl<sub>2</sub> were added, and the mixture was incubated at 25 °C for 2 h. To address the low solubility of the substrate, the mixture was further incubated at 37 °C for an additional hour. Afterwards, dephosphorylation using the BAP enzyme was performed at 37 °C for another hour. The reaction product was subjected to a C-18 SPE column, yielding a semi-purified product sufficient for NMR analysis. A single HPLC purification using a C-18 column enabled the isolation of GBL (**10**). The isolated product (**10d**) was fully characterized *via* 1D- and 2D-NMR analyses (Fig. S91–S95, ESI<sup>†</sup>). The yield of the isolated compound was approximately 30% (2.6 mg per single batch) when the *n*-C-5-SNAC (**6d**) substrate was used, with a total reaction time of approximately 4 h. This method was also applied to *n*-C-6, *n*-C-7, *iso*-C-5 and *iso*-C-7  $\beta$ -ketoacyl-SNACs (**6e**, **6f**, **6k**, and **6l**), and their structures and purity were confirmed by NMR (Fig. S96–S108, ESI<sup>†</sup>). The NMR spectra of natural compound **4** and the enzymatically synthesized *n*-C-7 GBL were identical (**10f**, Fig. S102, ESI<sup>†</sup>). Although organic synthesis of these GBL compounds has been reported previously,<sup>27,35,39,71</sup> this chemoenzymatic synthesis method may offer a simpler and faster approach for synthesizing a variety of GBLs. Modifying the structure of the SNAC substrate, which can be prepared in 2–3 steps within a few days, would facilitate the efficient synthesis of structurally diverse GBLs.

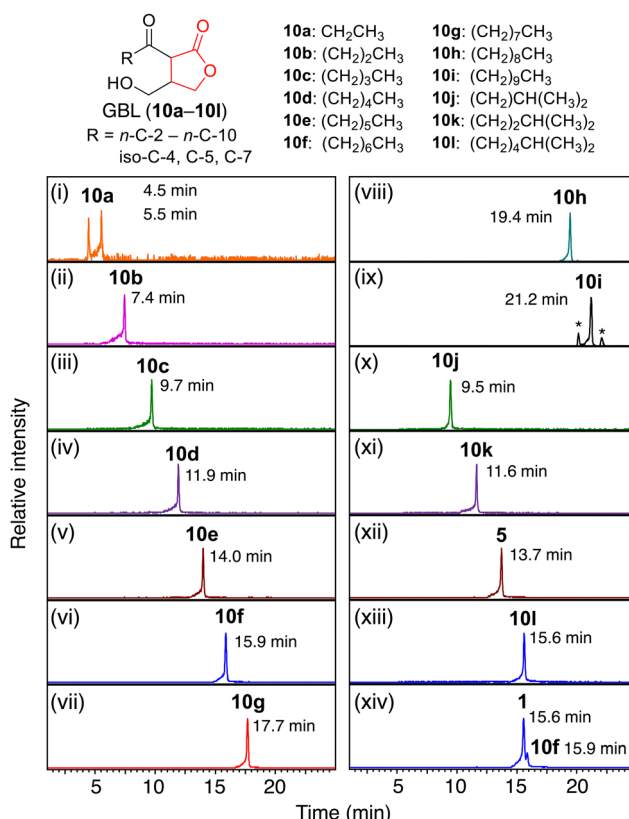


Fig. 4 Analysis of synthesized  $\gamma$ -butyrolactones (GBLs). HR-LCMS chromatograms of synthesized GBLs (**10a–10l**), (i)–(xi), (xiii)), isolated *iso*-C-6 GBL (**5**, (xii)) and the extract of *Streptomyces griseus* containing the A-factor (**1**) (xiv). Peaks marked with an asterisk are unrelated to GBL.

### Configurational analysis of enzymatic products

Horinouchi *et al.* first reported an *in vitro* BprA reaction and suggested the stereoselective reduction of butenolide based on a biological activity assay.<sup>29</sup> In this study, the low optical purity of the enzymatic product (**10d**) was indicated by the small Cotton effect in the CD spectrum. Hence, we investigated the chirality of the enzymatic products of GBLs using a chiral column chromatography. After the chiral column screening, four peaks estimated to be (3*R*)- and (3*S*)-*n*-C-5 GBL with keto-enol tautomers were detected in the enzymatic product (**10d**) *via* HPLC-DAD (Fig. 5(i), 254 nm, DAICEL CHIRALPAK AD-H). Fractionation and CD spectral analysis confirmed the separation of the (3*R*)- and (3*S*)-GBL enantiomers ((3*R*)-*n*-C-5 GBL; 285 nm,  $\Delta\epsilon + 0.643$ , 219 nm,  $\Delta\epsilon + 0.311$ , (3*S*)-*n*-C-5 GBL; 285 nm,

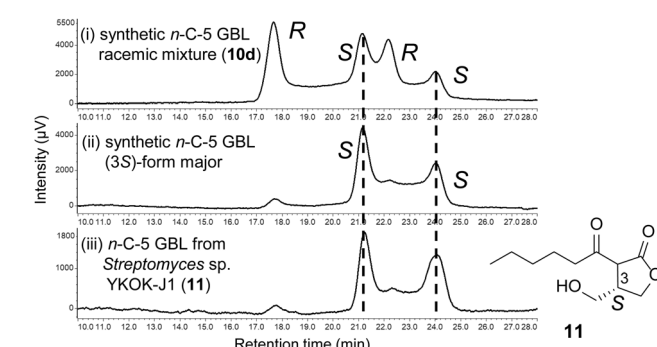


Fig. 5 Chiral HPLC chromatograms of *n*-C-5  $\gamma$ -butyrolactone (GBL). (i) Synthesized racemic *n*-C-5  $\gamma$ -butyrolactone (GBL) (**10d**), (ii) (3*S*)-form major synthetic *n*-C-5 GBL, and (iii) semipurified extract of *Streptomyces* sp. YKOK-J1 containing **11**.



$\Delta\varepsilon - 0.419$ , 219 nm,  $\Delta\varepsilon - 0.209$ ; Fig. S39 and S40, ESI<sup>†</sup>). The *n*-C-5 GBL (**10d**) synthesized using both MBP-BprA and tag-free BprA showed peaks with a ratio of  $(3R):(3S) = 62:38$ . This result suggested that the MBP tag did not affect the stereoselectivity of the product. The *n*-C-7 GBL (**10f**) synthesized using MBP-BprA showed the same ratio of  $(3R):(3S) = 62:38$ , whereas the natural *n*-C-7 GBL (**4**) isolated from *R. rhodnii* JCM 3203 exhibited a significantly higher  $(3R)$ -ratio ( $(3R):(3S) = 95:5$  (Fig. S41, ESI<sup>†</sup>)). Using the substrate iso-C-7  $\beta$ -ketooacyl-SNAC, which has the genuine acyl chain structure of BprA, the selectivity was slightly improved, but the product still consisted of a mixture of enantiomers ( $(3R):(3S) = 72:28$ , Fig. S42, ESI<sup>†</sup>).

The stereochemistry at C-3 should be established during the reduction of butenolide by BprA. To improve stereoselectivity, we attempted to identify BprA homologues capable of achieving high stereoselectivity. *bprA* is occasionally found in close proximity to *afsA*, as observed in *Streptomyces griseus*,<sup>29</sup> *S. coelicolor* A3(2),<sup>45</sup> *S. venezuelae* (JadW2),<sup>72</sup> and *S. virginiae* (BarS2)<sup>73</sup> (Fig. 1). In *Streptomyces* sp. YKOK-J1, the *sj-afsA* and *bprA* homologues (*sj-bprA*) are located in opposite directions (Fig. 1). Additionally, an *afsA* homologue was identified in *Streptomyces* sp. YKOK-I1 (*si-afsA*) through BLAST searches. No corresponding *bprA* homologue was found in the flanking region of *rr-afsA* and *si-afsA*, despite the high  $(3R)$ -enantiomeric ratio observed in the GBL compounds isolated from *R. rhodnii* JCM 3203 and *Streptomyces* sp. YKOK-I1 (2–5). Possible butenolide reductases were found in these strains *via* BLAST searches (*rr-bprA* and *si-bprA*), although these candidates were located far from *afsA* homologues. To test these candidates, SJ-BprA, Rr-BprA, and SI-BprA were expressed in *E. coli*. An enzymatic assay with MBP-Rr-AfsA and Rr-BprA showed only a trace product peak of *n*-C-7 GBL phosphate (**9f**) in the LCMS data. Similarly, an enzymatic assay using MBP-SJ-AfsA and SI-BprA produced only a trace product peak of *n*-C-5 GBL phosphate (**9d**) in the LCMS data. MBP-SJ-BprA exhibited a low conversion rate (approximately 20%), and the TEV protease was unable to effectively cleave the MBP tag from the fusion protein. Therefore, SJ-BprA was expressed without an MBP tag, although the yield of soluble protein was low. Eventually, SJ-BprA fully catalysed the conversion of *n*-C-5 butenolide phosphate (**8d**) into GBL phosphate (**9d**). The enzymatically produced GBL (**10d**) using SJ-BprA was analysed using chiral HPLC-DAD. Unexpectedly, the product exhibited a higher  $(3S)$ -enantiomeric ratio ( $(3R):(3S) = 37:63$ , Fig. S43, ESI<sup>†</sup>). Thus, high stereoselectivity in the reduction of butenolide phosphate could not be achieved *in vitro* in this study. The isolated natural compounds did not exhibit 100% optical purity. It is possible that racemization through intramolecular transesterification, as observed in the GBL synthesis process,<sup>35</sup> might have occurred to a very small extent within the actinomycete cells or during the isolation process.

### Identification of natural $(3S)$ -isomer of GBL

The stereochemistry at the C-3 position of GBL has been suggested to be crucial for its biological activity. To date, all unambiguously determined GBLs have been reported to have

$(3R)$  stereochemistry. Although  $(3S)$ -form GBL compounds were described in early studies, no experimental evidence, such as optical rotation data, CD spectra, or results of chiral column analysis using authentic standards, was provided. In this study, SJ-BprA was found to produce GBL with a relatively high proportion of the  $(3S)$ -isomer, leading us to investigate the absolute stereochemistry of GBL produced by *Streptomyces* sp. YKOK-J1. LCMS analysis indicated the presence of *n*-C-5 GBL in this strain (Fig. 6c and Fig. S48, ESI<sup>†</sup>). To confirm the stereochemistry, *n*-C-5 GBL (**11**) was extracted with acetone from a total of 255 mL of culture of *Streptomyces* sp. YKOK-J1 fermented with resin. The extract was purified using Strata C18-E, and the fractions containing *n*-C-5 GBL (**11**) were further purified using an Inert-Sustain C-18 column. The purified *n*-C-5 GBL was then analysed using chiral HPLC-DAD, along with standards of  $(3S)$ -*n*-C-5 GBL and racemic *n*-C-5 GBL. The purified *n*-C-5 GBL from *Streptomyces* sp. YKOK-J1 presented retention times identical to those of  $(3S)$ -*n*-C-5 GBL, with an enantiomeric ratio of  $(3R):(3S) = 1:9$  (Fig. 5). This study represents the first determination of a natural  $(3S)$ -form GBL from an actinomycete strain, which may expand the known chemical diversity of signalling molecules. Both enantiomers are present in animal pheromones such as olean and frontal, and their ratio can provide information about sex, age, and other characteristics.<sup>74,75</sup> The discovery of enantiomers in bacterial signalling molecules such as GBL, often referred to as “bacterial hormones”, is intriguing and may suggest a similarly complex role in microbial communication.

### GBL distribution in diverse actinomycete

With the isolated and synthetic GBL standards in hand, we investigated the presence of GBL compounds in various actinomycetes. Extracts from 31 actinomycete strains (Table 1 and Table S1, ESI<sup>†</sup>) were reanalyzed *via* HR-LCMS with 13 GBL standards (**5**, **10a–10l**). The results are summarized in Table 1. The A-factor, iso-C-7 GBL, was clearly detected in the extract of *Streptomyces griseus* at a retention time identical to that of the synthetic standard (**10l**), validating the accuracy of this analytical method (Fig. 4 (xiii, xiv)). Previously reported *n*-C-4 and *iso*-C-5 GBL (Sal-GBL1 and Sal-GBL2)<sup>15</sup> were confirmed in *Salinipora tropica*, and *iso*-C-4 GBL (**10b**) was newly identified as a natural product in this strain. The *n*-C-5, *n*-C-6, and *n*-C-10 GBLs (**10f**, **10e**, **10i**) were also newly identified as natural products in the genera *Rhodococcus* and/or *Streptomyces*. The *n*-C-7 GBL (**10f**) and *n*-C-9 GBL (**10h**) were detected in the genera *Dietzia*, *Nocardia*, *Gordonia*, *Rhodococcus*, and *Streptomyces* (Fig. 6a and b). Notably, the detection of GBLs in *Nocardia*, *Gordonia*, and *Dietzia* using HR-LCMS is reported here for the first time. The MSMS spectra of the detected GBLs (**10h**, **10f**) in these genera were identical to the spectra of their synthetic standards (Fig. 6d and e). This finding suggests that GBLs also function as signalling molecules in these genera of actinomycetes. These GBL-producing strains harbour *afsA* homologues with more than 30% AA similarity (Table 1). GBLs were not detected in the strains with low-similarity *afsA* homologues (<30% similarity), including *Mycobacterium cookii*, *Mycolicibacterium austroafricanum*, *Mycolicibacterium chlorophenolicum*,



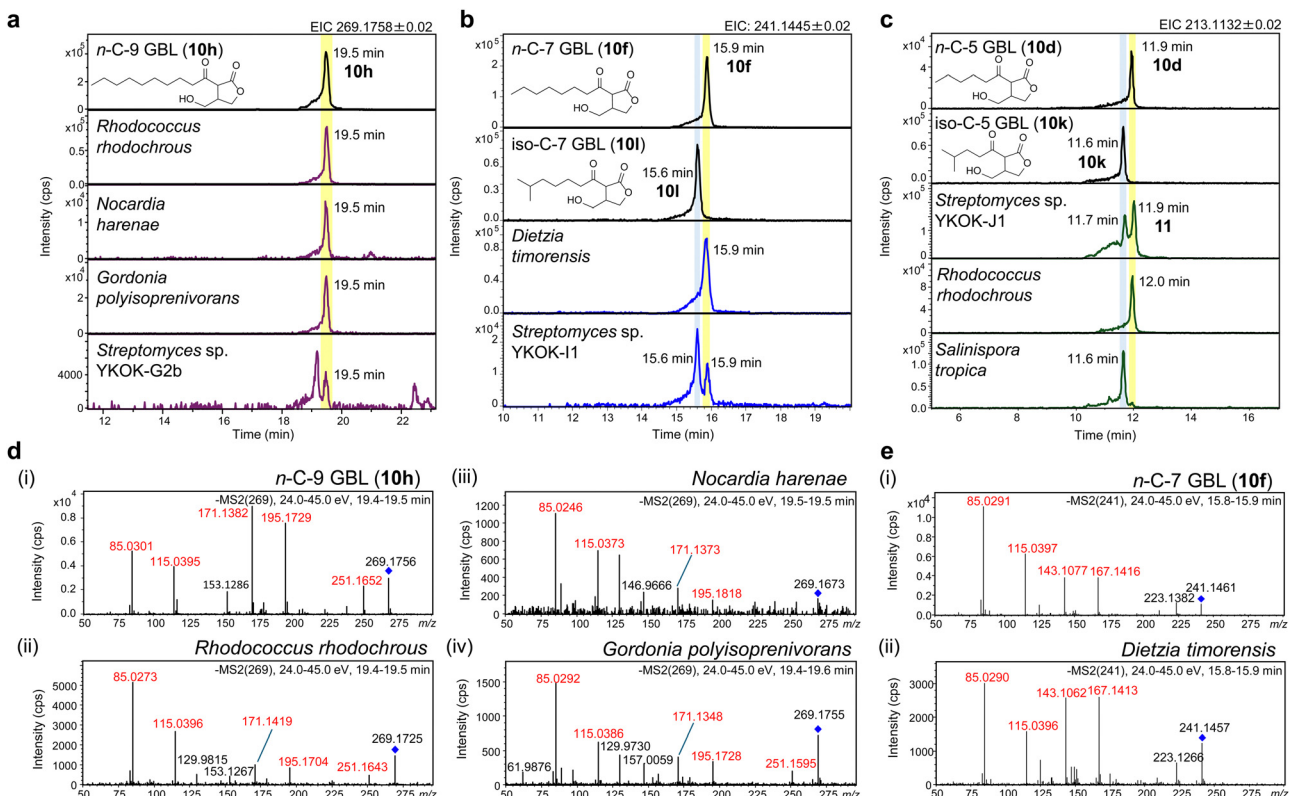


**Fig. 6** LCMS analysis of actinomycete strains. (a) HR-LCMS chromatograms of *n*-C-9 GBL (**10h**) and of *Rhodococcus rhodochrous*, *Nocardia hareniae*, *Gordonia polyisoprenivorans*, and *Streptomyces* sp. YKOK-G2b. (b) HR-LCMS chromatograms of *n*-C-7 GBL (**10f**), iso-C-7 GBL (**10l**), *Dietzia timorensis* and *Streptomyces* sp. YKOK-I1. (c) HR-LCMS chromatograms of *n*-C-5 GBL (**10d**), iso-C-5 GBL (**10k**), *Streptomyces* sp. YKOK-J1, and *Salinispora tropica*. (d) MSMS spectra of (i) *n*-C-9 GBL (**10h**) and of *m/z* 269 in (ii) *Rhodococcus rhodochrous*, (iii) *Nocardia hareniae*, and (iv) *Gordonia polyisoprenivorans*. (e) MSMS spectra of (i) *n*-C-7 GBL (**10f**) and of *m/z* 241 in (ii) *Dietzia timorensis*. The blue rhombuses denote the selected precursor ions. Characteristic fragment ions are indicated in red.

and *Streptomyces griseoaurantiacus*, although *Streptomyces* sp. YKOK-J1 exhibited the production GBLs (Table 1). Among the four *Rhodococcus* strains, only *R. erythropolis* did not produce detectable GBLs, probably due to the partial deletion of the hot-dog domain in its *afsA* homologue. While the presence of *afsA* homologues is a strong indicator of GBL production, GBLs were not detected in eight strains with plausible *afsA* homologues showing more than 30% AA similarity (Table 1). *n*-C-2 and *n*-C-3 GBL (**10a** and **10b**) were not detected in any of the tested strains, but the high volatility of these compounds may have led to their loss during culture and extraction. Overall, GBL compounds were detected in 15 out of 31 tested strains, representing 6 of the 10 tested genera (Table 1). These results revealed that various actinomycetes produce GBL compounds. Among the GBL-producing strains, seven strains contained *spt*-like gene clusters, but phosphotriester compounds were not detected in these strains by MS-guided screening of phosphotriester compounds focusing on their characteristic fragment ions, a method we developed.<sup>62</sup>

6-Hydroxy GBLs have been reported to be the major signalling molecules in *Streptomyces* species.<sup>11,26</sup> This study revealed that 6-keto GBLs are also distributed in *Streptomyces* species, although the known natural 6-keto GBLs are limited to examples such as the A-factor (**1**) in *S. griseus*. 6-Hydroxy GBLs are

biosynthesized from 6-keto GBLs *via* the reduction of a ketone at C-6.<sup>39,76</sup> The reduction of 6-keto GBLs (**10e**, **10l**) with NaBH<sub>4</sub> yielded a diastereomeric mixture of 6-hydroxy GBLs. Analysis of these 6-hydroxy GBLs revealed identical peaks in some actinomycete strains lacking 6-keto GBLs, such as the SCB-producing strains *Streptomyces coelicolor* A3(2) (*S. violaceoruber*) and *Streptomyces* sp. YKOK-D1 (Fig. S49–S53, ESI<sup>†</sup>). However, no possible 6-hydroxy GBLs were observed in the 15 actinomycete strains containing 6-keto GBLs. This observation suggested that the 6-keto GBLs detected in these strains were not biosynthetic precursors of 6-hydroxy GBL. Recent work by Parkinson *et al.* demonstrated the stereoselective synthesis of SCBs, which contain a (6*R*)-hydroxy group, from 6-keto GBLs *via* the ketoreductase ScbB.<sup>39</sup> Similarly, the stereoselective reduction of a ketone at C-6 to a hydroxy group was reported for BarS1, which produces virginiae butanolide A with a (6*S*)-hydroxy group.<sup>76</sup> These ketoreductases could be used to chemoenzymatically synthesize a series of 6-hydroxy GBLs.

In terms of chemical structure, this study expands the range of known side chain lengths of natural GBLs. Furthermore, the identification of (3*S*)-isomer of GBL highlights additional stereochemical diversity among natural GBLs. Bioinformatic analyses have revealed the widespread presence of *afsA* homologues across actinomycetes, suggesting that GBL compounds



are key signalling molecules.<sup>11</sup> However, only analytical chemistry can be used to determine their exact structures. This study provides formal evidence for the widespread occurrence of GBL compounds in actinomycete strains spanning multiple genera. Resin-assisted isolation involves simply adding commercially available resin to the culture, making it easily applicable to cultivable actinomycetes. Similarly, chemoenzymatic GBL synthesis can be reconstituted using AfsA and BprA. By applying analyses using GBL standards to a library of actinomycete extracts, valuable insights into the distribution of GBL can be obtained. The application of synthesized GBLs has significant potential for activating secondary metabolic pathways across these diverse actinomycetes. This approach could lead to the discovery of novel bioactive compounds and further expand our understanding of the chemical and biological diversity within this microbial group.

## Experimental

### Compound screening using LCMS

Bacteria were cultured with 2% starter culture in a 300 mL Erlenmeyer flask containing 50 mL of medium at 28 °C or 30 °C with shaking at 180 rpm using an EYELA MMS-3020 device. After 36–48 hours, sterile Amberlite XAD7HP resin (1 g, Sigma-Aldrich) was added to the flask, and fermentation was allowed to proceed for an additional 2–4 days. The cells and resin were collected by centrifugation at 4000×g for 10 min and then soaked in 50 mL of acetone for 30 min. After filtration *in vacuo*, the acetone extract was concentrated using a rotary evaporator. The resulting residue was dissolved in methanol (MeOH), and the solution was applied to a Strata C18-E SPE (2 g, Phenomenex) or Cosmosil 140C18-OPN column (1 g, 10 mm internal diameter (i.d.)). The column was then washed with three volumes of H<sub>2</sub>O, and eluate fractions were obtained using three volumes of H<sub>2</sub>O/MeOH (1:1, v/v), three volumes of H<sub>2</sub>O/MeOH (1:4, v/v), and four volumes of pure MeOH. Aliquots of the fractions were subjected to HR-LCMS analysis. HR-LCMS was performed using a Kinetex XB-C<sub>18</sub> column (2.6 µm, 4.6 mm i.d. × 100 mm, 100 Å, Phenomenex) with the following conditions: positive and negative mode, mobile phase A: 0.1% formic acid in H<sub>2</sub>O (v/v), mobile phase B: 0.1% formic acid in acetonitrile (MeCN) (v/v), 0.3 mL min<sup>-1</sup>, 0–25 min (20–100% B), 25–35 min (100% B), and 30 °C. The MS1 extracted ion chromatograms (EICs) corresponding to the GBLs were generated, and the molecular formula of each compound was determined on the basis of the high-resolution mass of the monoisotopic peaks.

### Identification of GBLs from actinomycetes

Extracts of the 31 strains of bacteria were analysed using HR-LCMS with the isolated and synthesized GBLs (5 and **10a–10l**). Actinomycete extracts prepared for compound screening were analysed under the same LCMS conditions. The molecular formulae of the detected compounds were determined on the basis of the high-resolution mass of monoisotopic peaks. Selected extracts were further analysed using LC-MSMS. MSMS

spectra of representative detected peaks in *Rhodococcus rhodochrous*, *Nocardia hareniae*, *Gordonia polyisoprenivorans* and *Dietzia timorensis* were analysed in automsms mode in otofControl with precursor ions: *m/z* 269 and 241 and a collision energy of 24–45 eV.

### One-pot chemoenzymatic reaction using AfsA, BprA, and BAP

The reaction mixture containing 2.5 to 12.5 µM MBP-SJ-AfsA, 10 mM *n*-C-5 β-ketoacyl-SNAC (**6d**), and 11 mM DHAP (**7**) was incubated in 1 or 2 mL of 50 mM McIlvaine buffer (pH 7.0) at 25 °C for 15 min. To this AfsA reaction, a BprA reaction mixture containing 5 µM BprA, 11 mM MgCl<sub>2</sub>, and 11 mM NADPH in an equal volume of 50 mM McIlvaine buffer (pH 7.0) was added, and the mixture was subsequently incubated at 25 °C for 2 h and 37 °C for 1 h. After adding 10× BAP buffer and BAP enzyme (10 units per mL), the mixture was incubated at 37 °C for 1 h. One volume of EtOH was added to the reaction mixture and then centrifuged at 18 000×g for 3 min to remove insoluble debris. The supernatants from several reaction batches were combined and evaporated *in vacuo*. The residue was applied to a Strata C18-E SPE column (2 g, Phenomenex), and then the column was washed with three volumes of H<sub>2</sub>O. The eluate fractions were obtained using three volumes of H<sub>2</sub>O/MeOH (4:1, v/v), three volumes of H<sub>2</sub>O/MeOH (1:1, v/v), three volumes of H<sub>2</sub>O/MeOH (1:4, v/v) and four volumes of pure MeOH. Fractions containing GBL were identified *via* ESI-MS and evaporated *in vacuo*. The resulting concentrate was applied to an InertSustain C18 column (10 mm i.d. × 250 mm, 5 µm, GL Sciences) with the following gradient conditions: mobile phase A, 0.1% formic acid in H<sub>2</sub>O; mobile phase B, 0.1% formic acid in MeCN; and gradient, 40% B, hold for 10 min, 40–70% B in 60 min, at a flow rate of 2.0 mL min<sup>-1</sup>. Compound elution was monitored by DAD and confirmed by ESI-MS. The structure and purity of **10d** were confirmed using NMR (Fig. S91–S95, ESI<sup>†</sup>). The pure compound **10d** in mg-scale was obtained within one day after initiating the one-pot reaction. The average isolated yield was 27.8% (23.3–30.8%, *n* = 6). Keto–enol tautomerization in GBLs caused a low yield during HPLC purification.

### Others

General experimental procedures, bacterial strains, isolation of GBLs from actinomycetes (2–5), purification of (3*S*)-*n*-C-5 GBL (**11**) from *Streptomyces* sp. YKOK-J1, chiral column analysis, NMR measurements, CD spectral measurements, synthesis of β-ketoacyl-SNAC (**6**), DHAP synthesis (**7**), docking study, isolation of *Streptomyces* sp. strains and their 16S rRNA sequence analysis and whole genome analysis, accession number, DNA synthesis, expression and purification of proteins, enzymatic reactions, reduction of C-6 ketone in GBLs were described in ESI.<sup>†</sup>

## Conclusions

Signalling molecules such as GBLs are pivotal regulators of secondary metabolism in actinomycetes, which are prolific sources for drug discovery. This study established two methodologies for the rapid identification of GBLs in actinomycetes.

The first approach utilizes coculture with an adsorbent resin, enabling the structural determination of GBLs (2–5) from small-scale cultures. The second approach involves the concise chemoenzymatic synthesis of 6-keto GBLs, which facilitates their identification across a broad range of actinomycetes *via* HR-LCMS. This study revealed the structural diversity of natural GBLs, including variations in side chain length and stereochemistry at the C-3 position. The methodologies developed here represent valuable tools for systematically identifying GBLs and will provide insights into their roles as signalling molecules. Furthermore, these findings contribute foundational knowledge for elucidating the regulatory mechanisms of secondary metabolism in actinomycetes, paving the way for harnessing these pathways to discover novel bioactive compounds.

## Author contributions

Conceptualization, methodology, investigation, visualization and writing – original draft by Y. K. resources and funding acquisition by Y. K. and M. Y.-Y. writing – review & editing by Y. K., M. Y.-Y. and K. K.

## Data availability

The data supporting this article have been included as part of the ESI.† NMR spectra, CD spectra, LCMS chromatograms, MS spectra, NMR tables, bacterial strain list, accession numbers, docking models, SDS-PAGE, Chiral HPLC chromatograms.

## Conflicts of interest

There are no conflicts to declare.

## Acknowledgements

This work was supported by the Japan Society for the Promotion of Science (JSPS) under KAKENHI Grant-in-Aid for Early-Career Scientists no. JP22K14833 and Grant-in-Aid for Scientific Research no. JP24K08723 to Y. K., and no. JP23H02146 and JP23K26839 to M. Y.-Y. This work was supported by Yazaki Memorial Foundation of Science and Technology and The Naito Foundation (to Y. K.). The authors thank Prof. T. Fujii, Graduate School of Agricultural Science, Tohoku University, for supporting the CD spectrum measurement using a JASCO J-700WI. pET28-MBP-TEV was a gift from Zita Balklava & Thomas Wassmer (Addgene plasmid #69929; <https://n2t.net/addgene:69929>). Bacterial strains were provided by Japan Collection of Microorganisms, RIKEN BRC which is participating in the National BioResource Project of the MEXT, Japan, and by the National Institute of Technology and Evaluation (NITE), NBRC (NITE Biological Resource Center). A part of this study was supported by Support system for young researchers to use research equipment, instruments, and devices in Tohoku University. Support from the FRIS CoRE, which is a shared research environment, is acknowledged.

## References

- E. A. Barka, P. Vatsa, L. Sanchez, N. Gaveau-Vaillant, C. Jacquard, J. P. Meier-Kolthoff, H.-P. Klenk, C. Clément, Y. Ouhdouch and G. P. van Wezel, *Microbiol. Mol. Biol. Rev.*, 2016, **80**, 1–43.
- G. P. van Wezel and K. J. McDowall, *Nat. Prod. Rep.*, 2011, **28**, 1311–1333.
- V. Fedorenko, O. Genilloud, L. Horbal, G. L. Marcone, F. Marinelli, Y. Paitan and E. Z. Ron, *BioMed Res. Int.*, 2015, **2015**, 591349.
- H. U. Van Der Heul, B. L. Bilyk, K. J. McDowall, R. F. Seipke and G. P. Van Wezel, *Nat. Prod. Rep.*, 2018, **35**, 575–604.
- S. Horinouchi, *Biosci., Biotechnol., Biochem.*, 2007, **71**, 283–299.
- S. Horinouchi and T. Beppu, *Proc. Jpn. Acad., Ser. B*, 2007, **83**, 277–295.
- S. Horinouchi and T. Beppu, *Mol. Microbiol.*, 1994, **12**, 859–864.
- E. Takano, T. Nihira, Y. Hara, J. J. Jones, C. J. Gershater, Y. Yamada and M. Bibb, *J. Biol. Chem.*, 2000, **275**, 11010–11016.
- N. H. Hsiao, S. Nakayama, M. E. Merlo, M. de Vries, R. Bunet, S. Kitani, T. Nihira and E. Takano, *Chem. Biol.*, 2009, **16**, 951–960.
- J. D. Sidda, V. Poon, L. Song, W. Wang, K. Yang and C. Corre, *Org. Biomol. Chem.*, 2016, **14**, 6390–6393.
- K. E. Creamer, Y. Kudo, B. S. Moore and P. R. Jensen, *Microb. Genomics*, 2021, **7**, 1–14.
- K. Arakawa, N. Tsuda, A. Taniguchi and H. Kinashi, *Chem-BioChem*, 2012, **13**, 1447–1457.
- C. Corre, L. Song, S. O'Rourke, K. F. Chater and G. L. Challis, *Proc. Natl. Acad. Sci. U. S. A.*, 2008, **105**, 17510–17515.
- S. Kitani, K. T. Miyamoto, S. Takamatsu, E. Herawati, H. Iguchi, K. Nishitomi, M. Uchida, T. Nagamitsu, S. Omura, H. Ikeda and T. Nihira, *Proc. Natl. Acad. Sci. U. S. A.*, 2011, **108**, 16410–16415.
- Y. Kudo, T. Awakawa, Y. L. Du, P. A. Jordan, K. E. Creamer, P. R. Jensen, R. G. Linington, K. S. Ryan and B. S. Moore, *ACS Chem. Biol.*, 2020, **15**, 3253–3261.
- A. Ceniceros, L. Dijkhuizen and M. Petrusma, *Sci. Rep.*, 2017, **7**, 17743.
- T. Kawaguchi, T. Asahi, T. Satoh, T. Uozumi and T. Beppu, *J. Antibiot.*, 1984, **37**, 1587–1595.
- I. Kapoor, P. Olivares and S. K. Nair, *eLife*, 2020, **9**, e57824.
- S. Zhou, H. Bhukya, N. Malet, P. J. Harrison, D. Rea, M. J. Belousoff, H. Venugopal, P. K. Sydor, K. M. Styles, L. Song, M. J. Cryle, L. M. Alkhalfaf, V. Fülop, G. L. Challis and C. Corre, *Nature*, 2021, **590**, 463–467.
- E. Takano, *Curr. Opin. Microbiol.*, 2006, **9**, 287–294.
- K. Arakawa, *Biosci., Biotechnol., Biochem.*, 2014, **78**, 183–189.
- O. Hara and T. Beppu, *J. Antibiot.*, 1982, **35**, 349–358.
- H. Ohashi, Y.-H. Zheng, T. Nihira and Y. Yamada, *J. Antibiot.*, 1989, **42**, 1191–1195.
- K. Hashimoto, T. Nihira and Y. Yamada, *J. Ferment. Bioeng.*, 1992, **73**, 61–65.



25 Y. Yamada, *Nippon Hosenkin Gakkaishi*, 1995, **9**, 57–65.

26 A. V. Polkade, S. S. Mantri, U. J. Patwekar and K. Jangid, *Front. Microbiol.*, 2016, **7**, 131.

27 Y. Yamada, K. Sugamura, M. Kondo, H. Yanagimoto and H. Okada, *J. Antibiot.*, 1987, **40**, 496–504.

28 K. Sato, T. Nihira, S. Sakuda, M. Yanagimoto and Y. Yamada, *J. Ferment. Bioeng.*, 1989, **68**, 170–173.

29 J.-Y. Kato, N. Funa, H. Watanabe, Y. Ohnishi and S. Horinouchi, *Proc. Natl. Acad. Sci. U. S. A.*, 2007, **104**, 2378–2383.

30 N. H. Hsiao, J. Söding, D. Linke, C. Lange, C. Hertweck, W. Wohlleben and E. Takano, *Microbiology*, 2007, **153**, 1394–1404.

31 S. Zhou, N. R. Malet, L. Song, C. Corre and G. L. Challis, *Chem. Commun.*, 2020, **56**, 14443–14446.

32 C. Schlawis, S. Kern, Y. Kudo, J. Grunenberg, B. S. Moore and S. Schulz, *Angew. Chem., Int. Ed.*, 2018, **57**, 14921–14925.

33 C. Schlawis, T. Harig, S. Ehlers, D. G. Guillen-Matus, K. E. Creamer, P. Jensen and S. Schulz, *ChemBioChem*, 2020, **21**, 1629–1632.

34 K. Jerye, H. Lüken, A. Steffen, C. Schlawis, L. Jänsch, S. Schulz and M. Brönstrup, *Adv. Sci.*, 2024, **11**, e2309515.

35 K. Mori, *Tetrahedron Lett.*, 1981, **22**, 3431–3432.

36 K. Mori and K. Yamane, *Tetrahedron*, 1982, **38**, 2919–2921.

37 K. Mori, *Tetrahedron*, 1983, **39**, 3107–3109.

38 J. B. Morin, K. L. Adams and J. K. Sello, *Org. Biomol. Chem.*, 2012, **10**, 1517–1520.

39 L. E. Wilbanks, H. E. Hennigan, C. D. Martinez-Brokaw, H. Lakkis, S. Thormann, A. S. Eggly, G. Buechel and E. I. Parkinson, *ACS Chem. Biol.*, 2023, **18**, 1624–1631.

40 Y. Zhang, M. Wang, J. Tian, J. Liu, Z. Guo, W. Tang and Y. Chen, *Appl. Microbiol. Biotechnol.*, 2020, **104**, 1695–1705.

41 T. B. Nguyen, S. Kitani, S. Shimma and T. Nihira, *Appl. Environ. Microbiol.*, 2018, **84**, e02791–17.

42 X. Liu, W. Wang, J. Li, Y. Li, J. Zhang and H. Tan, *Sci. China: Life Sci.*, 2021, **64**, 1575–1589.

43 A. van der Meij, S. S. Elsayed, C. Du, J. Willemse, T. M. Wood, N. I. Martin, J. M. Raaijmakers and G. P. van Wezel, *Appl. Environ. Microbiol.*, 2023, **89**, e0123923.

44 M. Biarnes-Carrera, R. Breitling and E. Takano, *Curr. Opin. Chem. Biol.*, 2015, **28**, 91–98.

45 M. Biarnes-Carrera, C.-K. Lee, T. Nihira, R. Breitling and E. Takano, *ACS Synth. Biol.*, 2018, **7**, 1043–1055.

46 J. E. Bowyer, E. Lc de Los Santos, K. M. Styles, A. Fullwood, C. Corre and D. G. Bates, *J. Biol. Eng.*, 2017, **11**, 30.

47 R. H. Feling, G. O. Buchanan, T. J. Mincer, C. A. Kauffman, P. R. Jensen and W. Fenical, *Angew. Chem., Int. Ed.*, 2003, **42**, 355–357.

48 K. D. Bauman, V. V. Shende, P. Y. T. Chen, D. B. B. Trivella, T. A. M. Gulder, S. Vellalath, D. Romo and B. S. Moore, *Nat. Chem. Biol.*, 2022, **18**, 538–546.

49 D. E. Nettleton, T. W. Doyle, B. Krishnan, G. K. Matsumoto and J. Clardy, *Tetrahedron Lett.*, 1985, **26**, 4011–4014.

50 Y. Inahashi, M. Iwatsuki, A. Ishiyama, A. Matsumoto, T. Hirose, J. Oshita, T. Sunazuka, W. Panbangred, Y. Takahashi, M. Kaiser, K. Otoguro and S. Ōmura, *Org. Lett.*, 2015, **17**, 864–867.

51 Y. Inahashi, T. Shiraishi, A. Také, A. Matsumoto, Y. Takahashi, S. Ōmura, T. Kuzuyama and T. Nakashima, *J. Antibiot.*, 2018, **71**, 749–752.

52 S. Hoshino, H. Onaka and I. Abe, *J. Ind. Microbiol. Biotechnol.*, 2019, **46**, 363–374.

53 J. J. Zhang, X. Tang and B. S. Moore, *Nat. Prod. Rep.*, 2019, **36**, 1313–1332.

54 D. Xue, Z. Shang, E. A. Older, Z. Zhong, C. Pulliam, K. Peter, M. Nagarkatti, P. Nagarkatti, Y.-X. Li and J. Li, *ACS Chem. Biol.*, 2023, **18**, 508–517.

55 C. Pulliam, D. Xue, A. Campbell, E. Older and J. Li, *Chem-BioChem*, 2024, **25**, e2024005.

56 S. Arsin, M. Pollari, E. Delbaje, J. Jokela, M. Wahlsten, P. Permi and D. Fewer, *RSC Chem. Biol.*, 2024, **5**, 1035–1044.

57 S. Komatsu, C. Tsumori, K. Ohnishi and K. Kai, *ACS Chem. Biol.*, 2020, **15**, 2860–2865.

58 Y. Kudo, C. T. Hanifin, Y. Kotaki and M. Yotsu-Yamashita, *J. Nat. Prod.*, 2020, **83**, 2706–2717.

59 Y. Kudo, C. T. Hanifin and M. Yotsu-Yamashita, *Org. Lett.*, 2021, **23**, 3513–3517.

60 F. Schalk, J. Fricke, S. Um, B. H. Conlon, H. Maus, N. Jäger, T. Heinzel, T. Schirmeister, M. Poulsen and C. Beemelmanns, *RSC Adv.*, 2021, **11**, 18748–18756.

61 G. C. A. Amos, T. Awakawa, R. N. Tuttle, A. C. Letzel, M. C. Kim, Y. Kudo, W. Fenical, B. S. Moore and P. R. Jensen, *Proc. Natl. Acad. Sci. U. S. A.*, 2017, **114**, E11121–E11130.

62 Y. Kudo, K. Konoki and M. Yotsu-Yamashita, *Biosci., Biotechnol., Biochem.*, 2022, **86**, 1333–1342.

63 N. Shikura, T. Nihira and Y. Yamada, *FEMS Microbiol. Lett.*, 1999, **171**, 183–189.

64 S. Galanie, D. Entwistle and J. Lalonde, *Nat. Prod. Rep.*, 2020, **37**, 1122–1143.

65 M. Hall, *RSC Chem. Biol.*, 2021, **2**, 958–989.

66 N. Cardullo, V. Muccilli and C. Tringali, *RSC Chem. Biol.*, 2022, **3**, 614–647.

67 O. Trott and A. J. Olson, *J. Comput. Chem.*, 2010, **31**, 455–461.

68 J. Eberhardt, D. Santos-Martins, A. F. Tillack and S. Forli, *J. Chem. Inf. Model.*, 2021, **61**, 3891–3898.

69 M. Mirdita, K. Schütze, Y. Moriwaki, L. Heo, S. Ovchinnikov and M. Steinegger, *Nat. Methods*, 2022, **19**, 679–682.

70 H. Currinn, B. Guscott, Z. Balklava, A. Rothnie and T. Wassmer, *Cell. Mol. Life Sci.*, 2016, **73**, 393–408.

71 J. B. Davis, J. D. Bailey and J. K. Sello, *Org. Lett.*, 2009, **11**, 2984–2987.

72 L. Wang and L. C. Vining, *Microbiology*, 2003, **149**, 1991–2004.

73 Y. J. Lee, S. Kitani, H. Kinoshita and T. Nihira, *Arch. Microbiol.*, 2008, **189**, 429.

74 G. Haniotakis, W. Francke, K. Mori, H. Redlich and V. Schurig, *J. Chem. Ecol.*, 1986, **12**, 1559–1568.

75 L. Rasmussen and D. Greenwood, *Chem. Senses*, 2003, **28**, 433–446.

76 N. Shikura, J. Yamamura and T. Nihira, *J. Bacteriol.*, 2002, **184**, 5151–5157.

